24th IMEKO TC4 International Symposium
22nd International Workshop on ADC and DAC Modelling and Testing
IMEKO TC-4 2020
Palermo, Italy, September 14-16, 2020

Effect of cross-talk on conditional measurements performed with multi-pixel photon counters

Giovanni Chesi[1], Alessia Allevi[2], Maria Bondani[3]

[1]*Department of Science and High Technology, University of Insubria, Via Valleggio 11, I-22100 Como, Italy, gchesi@uninsubria.it , present address: National Institute for Nuclear Physics, INFN, Via Bassi 6, 27100 Pavia, Italy*
[2]*Department of Science and High Technology, University of Insubria, and Institute for Photonics and Nanotechnologies, IFN-CNR, Como (Italy), alessia.allevi@uninsubria.it*
[3]*Institute for Photonics and Nanotechnologies, IFN-CNR, Via Valleggio 11, I-22100 Como, Italy, maria.bondani@uninsubria.it*

***Abstract* – We investigate the role of the optical cross-talk in the conditional measurements performed on quantum states of light. In particular, we analyze how the statistics of the conditional states are affected by cross-talk by retrieving their first and second moments and we test the sub-Poissonianity of the state by evaluating the Fano factor.**

I. INTRODUCTION

Conditional measurements are a well-known strategy for generating nonclassical states. As for quantum optical states, the nonlinear dynamics achieved by exploiting the reduction postulate has been largely investigated in many schemes, involving single-photon and time-multiplexed-photon-resolving detectors in the low energy regime [1, 2, 3, 4, 5, 6, 7], but also photon-number-resolving detectors in the mesoscopic regime [8, 9]. Specifically, for what concerns this last case, it has been proved that conditional measurements can be successfully performed by multi-pixel photon counters. Recently, we have shown [10, 11] that this is the case for Silicon Photomultipliers (SiPM), a class of cheap and portable Silicon-based photon-number-resolving detectors [12, 13, 14]. They are basically a matrix of single-photon avalanche diodes, working in Geiger-Muller regime. In our experiment, we generated a twin-beam (TWB) state via parametric down conversion, measured the photon-number observable on one of the two parties of the TWB state and selected the corresponding value on the other party, which is a standard procedure to generate sub-Poissonian conditional states. We found out that these commercial devices could detect the nonclassicality of such states. Thus, we concluded that SiPMs can be used for Quantum Optics applications. However, they are affected by spurious effects which could be critical for conditional measurements. The most detrimental spurious effect is known as Optical Cross-Talk (OCT) [15]. It consists in the emission of secondary infrared photons inside the silicon substrate once an avalanche process is generated in a cell by a detection event. The secondary photons may start a new avalanche in a neighbouring cell, thus yielding a spurious count. Note that the OCT is a common feature of the whole multi-pixel-photon-counter class, including cameras. Here we deal with a theoretical analysis of the OCT effects on conditional measurements. In particular, we focus on the case of single-mode input radiation. Our model provides closed formulas for the detection probabilities and for the statistics of conditional states. Moreover, our results can be directly compared with experimental data since they are based on experimentally accessible quantities.

In Sect. ii. we briefly introduce a general description of conditional measurements performed with photon-number-resolving detectors on single-mode TWB states and we extend it by including the OCT. Then, in Sect. iii., we retrieve the analytic expressions for the first moment and the Fano factor of the conditional state in the presence of the OCT. The Fano factor, which, for the photon-number observable $\hat{n}$, is defined as

$$F \equiv \frac{\langle \Delta \hat{n}^2 \rangle}{\langle \hat{n} \rangle} = \frac{\langle \hat{n}^2 \rangle - \langle \hat{n} \rangle^2}{\langle \hat{n} \rangle}, \tag{1}$$

can be used as a test of nonclassicality. Indeed, for $F < 1$, the statistics of the radiation field is, by definition, sub-Poissonian. Finally, in Sect. iv. we draw our conclusions.

II. CONDITIONAL MEASUREMENTS WITH SINGLE-MODE SQUEEZED STATES AND PHOTON-NUMBER-RESOLVING DETECTORS

As mentioned in the Introduction, here we deal with single-mode TWB states of light, i.e. bipartite entangled states of the form [16]

$$|\lambda\rangle\rangle = \sqrt{1-\lambda^2} \sum_n \lambda^n |n\rangle |n\rangle \tag{2}$$

where

$$\lambda^2 \equiv \frac{N}{N+1}.$$

and $N \equiv \langle \hat{n} \rangle$ is the mean number of photons in each beam. The conditioning measurement is performed on one of the

two parties of the entangled state, typically named as *idler*, so that the other party, the so-called *signal*, is correspondingly reduced accordingly with Born's rule.
In the absence of OCT, the positive-operator valued measure (POVM) describing a direct measure of the photon-number operator $\hat{n}$ over single-mode radiation reads [8]

$$\hat{\Pi}_m(\eta) = \left(\frac{\eta}{1-\eta}\right)^m \sum_{n=m}^{\infty} \binom{n}{m} (1-\eta)^n |n\rangle\langle n| \quad (3)$$

where m is the number of detected photons and η is the quantum efficiency of the detector. The effect of OCT can be included by considering the probability ε that an avalanche triggers a second *single* spurious avalanche firing a different cell [17, 18]. Thus, the number of cells fired by spurious avalanches cannot be larger than the number of the proper light events, which implies that, for the overall number of detected photons k, we have $m \leq k \leq 2m \Rightarrow k/2 \leq m \leq k$. Then, the POVM in Eq. (3) can be generalized as follows [18]

$$\hat{\Pi}_k(\eta,\varepsilon) = \left(\frac{\varepsilon}{1-\varepsilon}\right)^k \sum_{m=\lceil k/2 \rceil}^{k} \binom{m}{k-m} \left[\frac{(1-\varepsilon)^2}{\varepsilon}\right]^m \left(\frac{\eta}{1-\eta}\right)^m \sum_{n=m}^{\infty} \binom{n}{m} (1-\eta)^n |n\rangle\langle n|. \quad (4)$$

We remark that for the sake of simplicity we are assuming that the two detectors share the same parameter values, i.e. $\varepsilon_s = \varepsilon_i = \varepsilon$ and $\eta_s = \eta_i = \eta$, where the subscripts stand for *signal* and *idler*. The joint probability of detecting k_i photons on the idler and k_s on the signal is given by

$$\begin{aligned} \mathrm{P}(k_s,k_i) &= \mathrm{Tr}_{s,i}\left[|\lambda\rangle\rangle\langle\langle\lambda|\hat{\Pi}_{k_s}\otimes\hat{\Pi}_{k_i}\right] \\ &= (1-\lambda^2)\left(\frac{\varepsilon}{1-\varepsilon}\right)^{k_s+k_i} \sum_{m_s=\lceil \frac{k_s}{2}\rceil}^{k_s} \sum_{m_i=\lceil \frac{k_i}{2}\rceil}^{k_i} \\ &\binom{m_s}{k_s-m_s}\binom{m_i}{k_i-m_i}\left[\frac{(1-\varepsilon)^2}{\varepsilon}\frac{\eta}{1-\eta}\right]^{m_s+m_i} \\ &\sum_{n=\max(m_s,m_i)}^{\infty}\binom{n}{m_s}\binom{n}{m_i}[\lambda(1-\eta)]^{2n}. \end{aligned} \quad (5)$$

The probability of measuring k_i photons on the idler without inspecting the outcome on the signal is the marginal of Eq. (5) and it is found to be

$$\begin{aligned} \mathrm{p}(k_i) &= \frac{(1-\lambda^2)[(1-\varepsilon)\eta\lambda^2]^{k_i}}{[1-\lambda^2(1-\eta)]^{k_i+1}} \sum_{l=0}^{\lfloor \frac{k_i}{2}\rfloor} \binom{k_i-l}{l} \\ &\left[\frac{\varepsilon[1-\lambda^2(1-\eta)]}{(1-\varepsilon)^2\eta\lambda^2}\right]^l \\ &= \frac{(1-\lambda^2)[(1-\varepsilon)\eta\lambda^2]^{k_i}}{[1-\lambda^2(1-\eta)]^{k_i+1}} \frac{\mathrm{F}_{k_i+1}(x)}{x} \end{aligned} \quad (6)$$

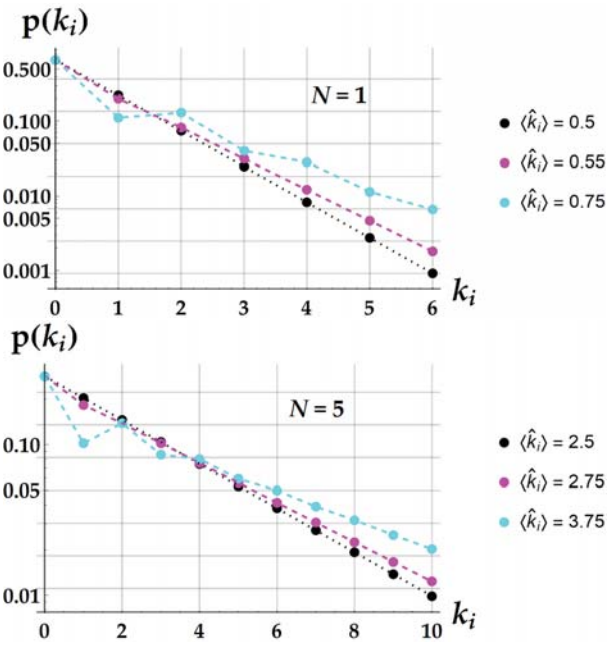

Fig. 1. Marginal probability of detecting k_i photons on the idler beam according to Eq. (6). The colors in each plot correspond to different values of the OCT probability ε. Black dots: $\varepsilon = 0$; magenta dots: $\varepsilon = 0.1$; cyan dots: $\varepsilon = 0.5$. The quantum efficiency η is set to 0.5. Note that the y-axis scale is logarithmic. The top panel shows the case $N = 1$. The bottom panel shows the case $N = 5$. The black dots are fitted by a thermal distribution, as expected.

where

$$x \equiv \sqrt{\frac{(1-\varepsilon)^2\eta\lambda^2}{\varepsilon[1-\lambda^2(1-\eta)]}}$$

and

$$\mathrm{F}_n(x) \equiv \frac{1}{2^n}\frac{\left(x+\sqrt{x^2+4}\right)^n - \left(x-\sqrt{x^2+4}\right)^n}{\sqrt{x^2+4}}$$

is the Fibonacci polynomial of order n. By using Eq. (6) to compute the mean value of the detected-photon-number distribution in the idler arm, one retrieves the well-known result $\langle\hat{k}_i\rangle = (1+\varepsilon)\eta\langle\hat{n}\rangle$ [18]. Moreover, the inspection and plot (see Fig. (1) of this marginal discrete distribution reveals that the effect of the OCT as described by this model is twofold.
First of all, for small numbers of detected photons, the OCT makes the even values more likely to be detected than the odd values. The reason is the following. Let m be the number of photons detected with probability η. As mentioned above, according to our OCT model, the outcome is a number k such that $m \leq k \leq 2m$. If m is odd, then $(m+1)/2$ of the possible values for k are odd and $(m+1)/2$ are even, but, if m is even, just $m/2$ of the possible values for k are odd while still $(m+1)/2$ are

even. This is basically due to the fact that $2m$, the superior boundary of k, is always even. Note that this asymmetry between even and odd outcomes tends to zero as m increases. The asymmetry is evident in the plots of Fig. (1), where the imbalance between $\mathrm{p}(1)$ and $\mathrm{p}(2)$ clearly modifies the thermal distribution typical of the no-OCT case (black dots).

Secondly, the OCT widens the detection-probability distribution. This is basically because the OCT, by definition, enhances the probability of getting larger outcomes by introducing spurious counts.

Provided that k_i photons are detected in the idler arm, the signal is correspondingly reduced to the conditional state

$$\begin{aligned}\hat{\rho}_s^{(k_i)} =& \frac{1}{\mathrm{p(k_i)}}\mathrm{Tr}_i[|\lambda\rangle\rangle\langle\langle\lambda|\hat{\mathbb{1}}_s \otimes \hat{\Pi}_{k_i}] \\ =& \frac{(1-\lambda^2)}{\mathrm{p(k_i)}}\left(\frac{\varepsilon}{1-\varepsilon}\right)^{k_i}\sum_{m_i=\left\lceil\frac{k_i}{2}\right\rceil}^{k_i}\binom{m_i}{k_i-m_i} \\ & \left[\frac{(1-\varepsilon)^2}{\varepsilon}\frac{\eta}{1-\eta}\right]^{m_i}\sum_{n=m_i}^{\infty}\binom{n}{m_i} \\ & [\lambda^2(1-\eta)]^n|n\rangle\langle n|.\end{aligned} \tag{7}$$

III. STATISTICS OF THE CONDITIONAL STATE

Given the conditional state in Eq. (7), the probability of detecting k_s photons in the signal arm having detected k_i photons in the idler one is retrieved from $\mathrm{Tr}_s[\hat{\rho}_s^{(k_i)}\hat{\Pi}_{k_s}]$, so that the generic n-th moment of this distribution is given by

$$\langle\widehat{k_s^n}\rangle^{(k_i)} = \sum_{k_s} k_s^n \mathrm{Tr}_s\left[\hat{\rho}_s^{(k_i)}\hat{\Pi}_{k_s}\right]. \tag{8}$$

Then the first moment of the conditional state distribution is straightforward and reads

$$\begin{aligned}\langle\hat{k}_s\rangle^{(k_i)} =& \mathrm{Tr}_s\left[\hat{\rho}_s^{(k_i)}\sum_{k_s}k_s\hat{\Pi}_{k_s}\right] = \\ =& \frac{\eta(1+\varepsilon)}{1-\lambda^2(1-\eta)}\left[k_i+\lambda^2(1-\eta)-\varepsilon A(x)\right]\end{aligned} \tag{9}$$

where

$$A(x) \equiv \frac{1-\lambda^2(1-\eta)}{\eta\lambda^2(1+\varepsilon)^2+4\varepsilon(1-\lambda^2)}\frac{k_i\mathrm{L}_{k_i}(x)-x\mathrm{F}_{k_i}(x)}{\mathrm{F}_{k_i+1}(x)}$$

is a combination of Fibonacci and Lucas polynomials. A Lucas polyinomial of order n is defined as follows

$$\mathrm{L}_n(x) \equiv \frac{1}{2^n}\left[\left(x+\sqrt{x^2+4}\right)^n+\left(x-\sqrt{x^2+4}\right)^n\right].$$

In Fig. (2) we show the mean value of the conditional-state as a function of the conditioning value k_i in the two cases already explored in Fig. (1). Again, in the two plots we note the effect of the imbalance between even and odd

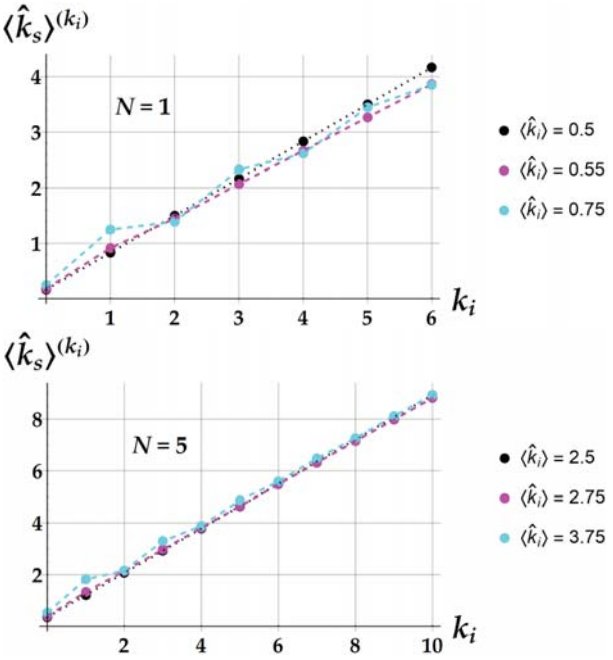

Fig. 2. Mean number of the conditional state as a function of the conditioning value k_i according to Eq. (9). The colors in each plot correspond to different values of the OCT probability ε. Black dots: $\varepsilon = 0$; magenta dots: $\varepsilon = 0.1$; cyan dots: $\varepsilon = 0.5$. The quantum efficiency η is set to 0.5. The top panel shows the case $N = 1$. The bottom panel shows the case $N = 5$.

detected numbers of photons. Furthermore, we remark that there is a threshold conditioning value $\tilde{k}_i$ such that the mean value of the conditional state in the presence of OCT is always larger than the same in the absence of OCT for $k_i < \tilde{k}_i$. This threshold value depends on the OCT probability, the mean value of the number of photons over the idler arm, the number of modes and the quantum efficiency. It can be observed in the case $N = 1$ (top panel).

The second moment is similarly found through Eq. (8) with $n = 2$. The first and the second moments of the conditional-state distribution allows to retrieve the Fano factor for the detected number of photons by means of Eq. (1) expressed for the operator $\hat{k}_s$. As mentioned above, the Fano factor provides a sufficient condition for nonclassicality. It reads

$$\begin{aligned}F^{(k_i)} =& \frac{1+3\varepsilon}{1+\varepsilon}-\eta(1+\varepsilon)+\frac{1}{\langle\hat{k}_s\rangle^{(k_i)}}\left[\frac{\eta(1+\varepsilon)}{1-\lambda^2(1-\eta)}\right]^2\cdot \\ & \left\{\lambda^2(1-\eta)(k_i+1)-\varepsilon A(x)\left[\lambda^2(1-\eta)+\varepsilon A(x)-B(x)\right]\right\}\end{aligned} \tag{10}$$

where

$$\begin{aligned}B(x) \equiv& \{k_i^2(x^2+4)\left[\mathrm{L}_{k_i}(x)-x\mathrm{F}_{k_i}(x)\right] \\ & +k_i\left[3x^2\mathrm{L}_{k_i}(x)-(x^2+4)x\mathrm{F}_{k_i}(x)\right]+2(x^2-2)x\mathrm{F}_{k_i}(x)\} \\ & \{2(x^2+4)\left[k_i\mathrm{L}_{k_i}(x)-x\mathrm{F}_{k_i}(x)\right]\}^{-1}\end{aligned}$$

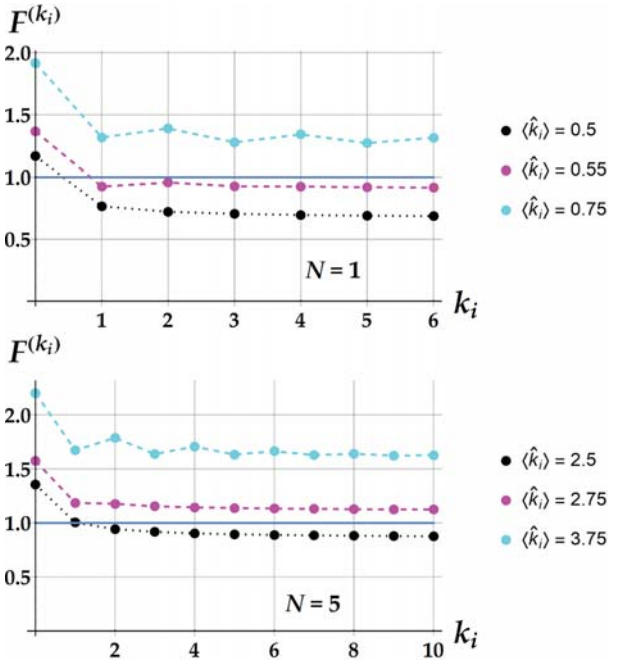

Fig. 3. Fano factor of the conditional state as a function of the conditioning value k_i according to Eq. (10). The colors in each plot correspond to different values of the OCT probability ε. Black dots: $\varepsilon = 0$; magenta dots: $\varepsilon = 0.1$; cyan dots: $\varepsilon = 0.5$. The quantum efficiency η is set to 0.5. The top panel shows the case $N = 1$. The bottom panel shows the case $N = 5$. The gray straight line highlights the Poissonian case, namely the threshold between sub- and super-Poissonian light.

is again a combination of Fibonacci and Lucas polynomials.

In Fig. 3 we plot the Fano factor of the conditional state in the cases $N = 1$ (top panel) and $N = 5$ (bottom panel). As expected, the effect of OCT implies a widening of the variance of the distribution with respect to the mean value, which is intrinsically detrimental to the sub-Poissonianity of the conditional-state statistics. Note that if ε is large enough, the detected light is not sub-Poissonian for any conditioning value.

Again, it is worth-noting that cyan lines in the two panels show evidence of the imbalance introduced by this OCT model on the even and odd conditioning values.

IV. CONCLUSIONS

The effect of the OCT on conditional measurements was here addressed by generalizing the POVM for photocounters in Eq. (3).

Moreover, we found out that the OCT, as described by our model, introduces an imbalance between even and odd detected-photon numbers.

The effects of this property on the conditonal-state statistics need further investigation. Furthermore, a generalization to the multi-mode case is required for a proper comparison with the recent experiment mentioned in the Introduction [10].

As a last remark, note that, upon substituing λ^2 with $\langle \hat{k}_i \rangle$, our results are all expressed in terms of measurable quantities and therefore amenable for direct experimental tests.

V. *

References

[1] M.Takeoka, M.Sasaki, “Conditional generation of an arbitrary superposition of coherent states", Phys. Rev. A, vol.75, June 2007, pp.1-4.

[2] O.Haderka, J.Peřina, Jr., M.Hamar, J.Peřina, “Direct measurement and reconstruction of nonclassical features of twin beams generated in spontaneous parametric down-conversion", Phys. Rev. A, vol.71, March 2005, pp.1-5.

[3] J.M.Raimond, M.Brune, S.Haroche, “Manipulating quantum entanglement with atoms and photons in a cavity", Rev. Mod. Phys., vol.73, August 2001, pp.565-582.

[4] M.S.Kim, E.Park, P.L.Knight, H.Jeong, “Nonclassicality of a photon-subtracted Gaussian field", Phys. Rev. A, vol.71, April 2005, pp.1-6.

[5] A.Ourjoumtsev, A.Dantan, R.Tualle-Brouri, P.Grangier, “Increasing entanglement between Gaussian states by coherent photon subtraction", Phys. Rev. Lett., vol.98, January 2007, pp.1-4.

[6] A.M.Branczyk, T.C.Ralph, W.Helwig, C.Silberhorn, “Optimized generation of heralded Fock states using parametric down-conversion", New J. Phys., vol.12, June 2010, pp.1-29.

[7] J.Peřina, Jr., O.Haderka, V.Michálek, “Sub-Poissonian-light generation by postselection from twin beams", Opt. Express, vol.21, No.16, August 2013, pp.19387-19394.

[8] A.Allevi, A.Andreoni, F.A.Beduini, M.Bondani, M.G.Genoni, S.Olivares, M.G.A.Paris, “Conditional measurements on multimode pairwise entangled states from spontaneous parametric downconversion”, EPL, vol.92, October 2010, pp.1-6.

[9] M.Lamperti, A.Allevi, M.Bondani, R.Machulka, V.Michálek, O.Haderka, J.Peřina, Jr., “Optimal sub-Poissonian light generation from twin beams by photon-number resolving detectors", J. Opt. Soc. Am. B, vol.31, No.1, January 2014, pp. 20-25.

[10] G.Chesi, L.Malinverno, A.Allevi, R.Santoro, M.Caccia, M.Bondani, “Measuring nonclassicality with silicon photomultipliers", Opt. Lett., vol.44, No.6, March 2019, pp. 1371-1374.

[11] G.Chesi, A.Allevi, M.Bondani, “Autocorrelation functions: a useful tool for both state and detector

characterisation", Quantum Meas. Quantum Metrol., vol.6, March 2019, pp.1-6.

[12] C.Piemonte, “A new Silicon Photomultiplier structure for blue light detection", Nuclear Instruments and Methods in Physics Research A, vol.568, August 2006, pp.224-232.

[13] R.Klanner, “Characterization of SiPMs", Nuclear Instruments and Methods in Physics Research Section A: Accelerators, Spectrometers, Detectors and Associated Equipment, vol.926, May 2019, pp.36-56.

[14] G.Chesi, L.Malinverno, A.Allevi, R.Santoro, M.Caccia, A.Martemiyanov, M.Bondani, “Optimizing Silicon photomultipliers for Quantum Optics", Sci.Rep., vol.9, April 2019, pp.1-12.

[15] F.Nagy, M.Mazzillo, L.Renna, G.Valvo, D.Sanfilippo, B.Carbone, A.Piana, G.Fallica, J.Molnár, “Afterpulse and delayed crosstalk analysis on a STMicroelectronics silicon photomultiplier", Nuclear Instruments and Methods in Physics Research, Section A: Accelerators, Spectrometers, Detectors and Associated Equipment, vol.759, September 2014, pp.44-49.

[16] A.Ferraro, S.Olivares, M.G.A.Paris, “Gaussian states in continuous variable quantum information", Bibliopolis, Napoli, Italy, 2005.

[17] I.Afek, A. Natan, O. Ambar, Y. Silberberg, “Quantum state measurements using multipixel photon detectors", Phys. Rev. A, vol.79, April 2009, pp.1-6.

[18] M.Ramilli, A.Allevi, V.Chmill, M.Bondani, M.Caccia, A.Andreoni, “Photon-number statistics with silicon photomultipliers", J. Opt. Soc. Am. B, vol. 27, May 2010, pp.852-862.